

Unique Properties and Reactivity of High-Valent Manganese—Oxo versus Manganese—Hydroxo in the Salen Platform

Takuya Kurahashi,[†] Akihiro Kikuchi,[‡] Yoshitsugu Shiro,[‡] Masahiko Hada,[§] and Hiroshi Fujii^{*†}

[†]*Institute for Molecular Science & Okazaki Institute for Integrative Bioscience, National Institutes of Natural Sciences, Myodaiji, Okazaki, Aichi 444-8787, Japan*, [‡]*RIKEN SPring-8 Center, Harima Institute, 1-1-1 Kouto, Sayo, Hyogo 679-5148, Japan*, and [§]*Department of Chemistry, Graduate School of Science, Tokyo Metropolitan University, 1-1 Minami-Osawa, Hachioji-shi, Tokyo 192-0397, Japan*

Received April 9, 2010

To gain an understanding of oxidation reactions by $\text{Mn}^{\text{III}}(\text{salen})$, a reaction of $\text{Mn}^{\text{III}}(\text{salen})$ with *m*-chloroperoxybenzoic acid in the absence of a substrate is investigated. UV–vis, perpendicular- and parallel-mode electron paramagnetic resonance, and X-ray absorption spectroscopy show that the resulting solution contains $\text{Mn}^{\text{IV}}(\text{salen})(\text{O})$ as a major product and $\text{Mn}^{\text{IV}}(\text{salen})(\text{OH})$ as a minor product. $\text{Mn}^{\text{IV}}(\text{salen})(\text{O})$ readily reacts with 4-*H*-2,6-*tert*-Bu₂C₆H₂OH (homolytic bond dissociation energy of an OH bond, $\text{BDE}_{\text{OH}} = 82.8 \text{ kcal mol}^{-1}$), 4-CH₃CO-2,6-*tert*-Bu₂C₆H₂OH ($\text{BDE}_{\text{OH}} = 83.1 \text{ kcal mol}^{-1}$), and 4-NC-2,6-*tert*-Bu₂C₆H₂OH ($\text{BDE}_{\text{OH}} = 84.2 \text{ kcal mol}^{-1}$) at 203 K, following second-order rate kinetics. $\text{Mn}^{\text{IV}}(\text{salen})(\text{OH})$ reacts with 4-CH₃CO-2,6-*tert*-Bu₂C₆H₂OH ($\text{BDE}_{\text{OH}} = 83.1 \text{ kcal mol}^{-1}$) much more slowly under identical conditions than $\text{Mn}^{\text{IV}}(\text{salen})(\text{O})$ and does not react with 4-NC-2,6-*tert*-Bu₂C₆H₂OH ($\text{BDE}_{\text{OH}} = 84.2 \text{ kcal mol}^{-1}$), suggesting that the thermodynamic hydrogen-atom-abstracting ability of $\text{Mn}^{\text{IV}}(\text{salen})(\text{OH})$ is about 83 kcal mol^{-1} . The rate constant for reactions of $\text{Mn}^{\text{IV}}(\text{salen})(\text{OH})$ with phenols is not dependent on the concentration of phenols, suggesting that $\text{Mn}^{\text{IV}}(\text{salen})(\text{OH})$ might bind phenols prior to the rate-limiting oxidation reactions. Quantum chemical calculations are carried out for $\text{Mn}^{\text{IV}}(\text{salen})(\text{O})$ and $\text{Mn}^{\text{IV}}(\text{salen})(\text{OH})$, both of which well reproduce the extended X-ray absorption fine structures as well as the electronic configurations. It is also indicated that protonation of $\text{Mn}^{\text{IV}}(\text{salen})(\text{OH})$ induces a drastic electronic structural change from manganese(IV) phenolate to a manganese(III) phenoxyl radical, which is also consistent with the experimental observation.

Introduction

High-valent manganese–oxo species have been the focus of extensive investigations because of their key role in synthetic

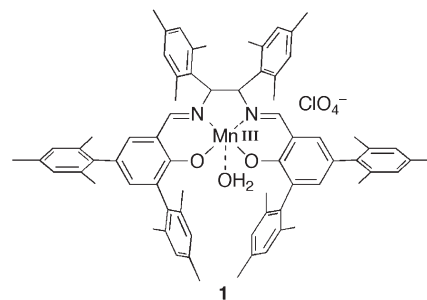
and biological oxidation reactions. The electronic structures and reactivity of $\text{Mn}^{\text{IV}}=\text{O}$ and $\text{Mn}^{\text{V}}=\text{O}$ species in various coordination environments have been actively investigated.^{1–9} However, less is known for a manganese salen complex, $\text{Mn}^{\text{III}}(\text{salen})$ (**1**), which was discovered by Kochi and co-workers as an excellent epoxidation catalyst¹⁰ and was then applied for catalytic enantioselective epoxidation of unfunctionalized olefins by Jacobsen and Katsuki.^{11,12} Kochi originally

- *To whom correspondence should be addressed. E-mail: hiro@ims.ac.jp.
(1) (a) McEvoy, J. P.; Brudvig, G. W. *Chem. Rev.* **2006**, *106*, 4455–4483. (b) Pecoraro, V. L.; Hsieh, W.-Y. *Inorg. Chem.* **2008**, *47*, 1765–1778.
(2) (a) Collins, T. J.; Gordon-Wylie, S. W. *J. Am. Chem. Soc.* **1989**, *111*, 4511–4513. (b) Collins, T. J.; Powell, R. D.; Slebochnick, C.; Uffelman, E. S. *J. Am. Chem. Soc.* **1990**, *112*, 899–901. (c) MacDonnell, F. M.; Fackler, N. L. P.; Stern, C.; O'Halloran, T. V. *J. Am. Chem. Soc.* **1994**, *116*, 7431–7432. (d) Miller, C. G.; Gordon-Wylie, S. W.; Horwitz, C. P.; Strazisar, S. A.; Peraino, D. K.; Clark, G. R.; Weintraub, S. T.; Collins, T. J. *J. Am. Chem. Soc.* **1998**, *120*, 11540–11541.
(3) (a) Groves, J. T.; Lee, J.; Marla, S. S. *J. Am. Chem. Soc.* **1997**, *119*, 6269–6273. (b) Jin, N.; Groves, J. T. *J. Am. Chem. Soc.* **1999**, *121*, 2923–2924. (c) Jin, N.; Bourassa, J. L.; Tizio, S. C.; Groves, J. T. *Angew. Chem., Int. Ed.* **2000**, *39*, 3849–3851. (d) Nam, W.; Kim, I.; Lim, M. H.; Choi, H. J.; Lee, J. S.; Jang, H. G. *Chem.—Eur. J.* **2002**, *8*, 2067–2071. (e) Zhang, R.; Newcomb, M. *J. Am. Chem. Soc.* **2003**, *125*, 12418–12419. (f) Zhang, R.; Homer, J. H.; Newcomb, M. *J. Am. Chem. Soc.* **2005**, *127*, 6573–6582. (g) De Angelis, F.; Jin, N.; Car, R.; Groves, J. T. *Inorg. Chem.* **2006**, *45*, 4268–4276. (h) Song, W. J.; Seo, M. S.; George, S. D.; Ohta, T.; Song, R.; Kang, M.-J.; Tosha, T.; Kitagawa, T.; Solomon, E. I.; Nam, W. *J. Am. Chem. Soc.* **2007**, *129*, 1268–1277. (i) Lahaye, D.; Groves, J. T. *J. Inorg. Biochem.* **2007**, *101*, 1786–1797. (j) Jin, N.; Ibrahim, M.; Spiro, T. G.; Groves, J. T. *J. Am. Chem. Soc.* **2007**, *129*, 12416–12417. (k) Gross, Z. *Angew. Chem., Int. Ed.* **2008**, *47*, 2737–2739. (l) Lee, J. Y.; Lee, Y.-M.; Kotani, H.; Nam, W.; Fukuzumi, S. *Chem. Commun.* **2009**, 704–706. (m) Crestoni, M. E.; Fornarini, S.; Lanucara, F. *Chem.—Eur. J.* **2009**, *15*, 7863–7866. (n) Arunkumar, C.; Lee, Y.-M.; Lee, J. Y.; Fukuzumi, S.; Nam, W. *Chem.—Eur. J.* **2009**, *15*, 11482–11489.

- (4) Shimazaki, Y.; Nagano, T.; Takesue, H.; Ye, B.-H.; Tani, F.; Naruta, Y. *Angew. Chem., Int. Ed.* **2004**, *43*, 98–100.
(5) (a) Groves, J. T.; Stern, M. K. *J. Am. Chem. Soc.* **1987**, *109*, 3812–3814. (b) Schappacher, M.; Weiss, R. *Inorg. Chem.* **1987**, *26*, 1190–1192. (c) Czernuszewicz, R. S.; Su, Y. O.; Stern, M. K.; Macor, K. A.; Kim, D.; Groves, J. T.; Spiro, T. G. *J. Am. Chem. Soc.* **1988**, *110*, 4158–4165. (d) Groves, J. T.; Stern, M. K. *J. Am. Chem. Soc.* **1988**, *110*, 8628–8638. (e) Arasasingham, R. D.; He, G.-X.; Bruice, T. C. *J. Am. Chem. Soc.* **1993**, *115*, 7985–7991. (f) Ayougou, K.; Bill, E.; Charnock, J. M.; Garner, C. D.; Mandon, D.; Trautwein, A. X.; Weiss, R.; Winkler, H. *Angew. Chem., Int. Ed. Engl.* **1995**, *34*, 343–346. (g) Fukuzumi, S.; Fujioka, N.; Kotani, H.; Ohkubo, K.; Lee, Y.-M.; Nam, W. *J. Am. Chem. Soc.* **2009**, *131*, 17127–17134.
(6) (a) Gross, Z.; Golubkov, G.; Simkhovich, L. *Angew. Chem., Int. Ed.* **2000**, *39*, 4045–4047. (b) Liu, H.-Y.; Lai, T.-S.; Yeung, L.-L.; Chang, C. K. *Org. Lett.* **2003**, *5*, 617–620. (c) Liu, H.-Y.; Zhou, H.; Liu, L.-Y.; Ying, X.; Jiang, H.-F.; Chang, C.-K. *Chem. Lett.* **2007**, *36*, 274–275. (d) Gao, Y.; Åkermark, T.; Liu, J.; Sun, L.; Åkermark, B. *J. Am. Chem. Soc.* **2009**, *131*, 8726–8727. (e) Liu, H.-Y.; Yam, F.; Xie, Y.-T.; Li, X.-Y.; Chang, C. K. *J. Am. Chem. Soc.* **2009**, *131*, 12890–12891.

postulated that reactions of **1** with oxidants such as NaOCl, PhIO, and *m*-chloroperoxybenzoic acid (*m*-CPBA) generate $\text{Mn}^{\text{V}}(\text{salen})(\text{O})$, which transfers the manganese-bound oxygen atom to olefins and regenerates **1**.¹⁰ The $\text{Mn}^{\text{V}}(\text{salen})(\text{O})$ model has been frequently employed in theoretical considerations to explain the selectivity in $\text{Mn}^{\text{III}}(\text{salen})$ -catalyzed enantioselective epoxidation.¹³ However, the experimental evidence for the existence of $\text{Mn}^{\text{V}}(\text{salen})(\text{O})$ is still limited, and the best evidence to date is detection of the ion signal for $\text{Mn}^{\text{V}}(\text{salen})(\text{O})$ by electrospray mass spectrometry.¹⁴ It has also been reported that a transient that could be assigned as $\text{Mn}^{\text{V}}(\text{salen})(\text{O})$ was detected via laser flash photolysis^{15a} and stopped-flow spectrophotometry.^{15b} However, electron paramagnetic resonance (EPR) and X-ray absorption spectroscopy (XAS) studies have shown that reactions of **1** with NaOCl, PhIO, and *m*-CPBA in the absence of a substrate result in mixtures of $\text{Mn}^{\text{IV}}(\text{salen})$ species that were not fully characterized.¹⁶ We recently reported the preparation of $\text{Mn}^{\text{IV}}(\text{salen})(\text{O})$ using a sterically hindered salen ligand (Chart 1), which was thoroughly characterized using various spectroscopic techniques.¹⁷

Another species to be considered is $\text{Mn}^{\text{IV}}(\text{salen})(\text{OH})$, which might be generated as a consequence of hydrogen-atom

Chart 1. Sterically Hindered **1**

abstraction by putative $\text{Mn}^{\text{V}}(\text{salen})(\text{O})$ or simply as a consequence of protonation of $\text{Mn}^{\text{IV}}(\text{salen})(\text{O})$. Such high-valent metal complexes carrying hydroxide are also an issue of interest. Green et al. reported that chloroperoxidase compound II has $\text{Fe}^{\text{IV}}\text{OH}$ rather than $\text{Fe}^{\text{IV}}=\text{O}$.¹⁸ They proposed that an axial thiolate ligation enhances the basicity of $\text{Fe}^{\text{IV}}=\text{O}$, which is a major driving force for thiolate-ligated compound I (formally $\text{Fe}^{\text{V}}=\text{O}$) to perform hydrogen-atom abstraction from inert substrates. Busch et al. prepared and crystallographically characterized a mononuclear Mn^{IV} complex containing a pair of hydroxo ligands in their ultrarigid ethylene cross-bridged macrocyclic ligand.¹⁹ Their $\text{Mn}^{\text{IV}}\text{OH}$ complex shows highly selective hydrogen-atom-abstrating ability, suggesting that high-valent metal hydroxo species may also play a role in catalytic oxidation reactions. The reactivities of $\text{Mn}^{\text{IV}}\text{OH}$ and $\text{Mn}^{\text{IV}}=\text{O}$ were investigated by comparing thermodynamic hydrogen-atom-abstrating abilities by means of the Bordwell/Mayer method^{20,21} as well as comparing activation barriers including both activation entropies and enthalpies. We also reported the preparation of $\text{Mn}^{\text{IV}}(\text{salen})(\text{OH})$ in our sterically hindered salen platform (Chart 1).¹⁷

We herein report the reaction of our sterically hindered **1** with *m*-CPBA, an oxidant that is employed for $\text{Mn}^{\text{III}}(\text{salen})$ -catalyzed oxidation,²² using the previously reported $\text{Mn}^{\text{IV}}(\text{salen})(\text{O})$ and $\text{Mn}^{\text{IV}}(\text{salen})(\text{OH})$ as reference complexes.¹⁷ It is expected that steric bulk incorporated to the salen ligand prevents dimerization, thus enabling us to focus on mononuclear high-valent species. UV-vis, perpendicular- and parallel-mode EPR, and XAS show that the resulting solution contains $\text{Mn}^{\text{IV}}(\text{salen})(\text{O})$ as a major product and $\text{Mn}^{\text{IV}}(\text{salen})(\text{OH})$ as a minor product. To compare the reactivities of $\text{Mn}^{\text{IV}}(\text{salen})(\text{O})$ and $\text{Mn}^{\text{IV}}(\text{salen})(\text{OH})$, we employ a series of substituted phenols as substrates for hydrogen-atom-abstraction reactions,²³ which suggest that their reaction pathways may

- (7) (a) Mandimutsira, B. S.; Ramdhanie, B.; Todd, R. C.; Wang, H.; Zareba, A. A.; Czernuszewicz, R. S.; Goldberg, D. P. *J. Am. Chem. Soc.* **2002**, *124*, 15170–15171. (b) Lansky, D. E.; Mandimutsira, B.; Ramdhanie, B.; Clausen, M.; Penner-Hahn, J.; Zvyagin, S. A.; Telser, J.; Krzystek, J.; Zhan, R.; Ou, Z.; Kadish, K. M.; Zakharov, L.; Rheingold, A. L.; Goldberg, D. P. *Inorg. Chem.* **2005**, *44*, 4485–4498. (c) Lansky, D. E.; Goldberg, D. P. *Inorg. Chem.* **2006**, *45*, 5119–5125.
- (8) (a) Parsell, T. H.; Behan, R. K.; Green, M. T.; Hendrich, M. P.; Borovik, A. S. *J. Am. Chem. Soc.* **2006**, *128*, 8728–8729. (b) Parsell, T. H.; Yang, M.-J.; Borovik, A. S. *J. Am. Chem. Soc.* **2009**, *131*, 2762–2763.
- (9) Khenkin, A. M.; Kumar, D.; Shaik, S.; Neumann, R. J. *Am. Chem. Soc.* **2006**, *128*, 15451–15460.
- (10) Srinivasan, K.; Michaud, P.; Kochi, J. K. *J. Am. Chem. Soc.* **1986**, *108*, 2309–2320.
- (11) (a) Zhang, W.; Loebach, J. L.; Wilson, S. R.; Jacobsen, E. N. *J. Am. Chem. Soc.* **1990**, *112*, 2801–2803. (b) Irie, R.; Noda, K.; Ito, Y.; Katsuki, T. *Tetrahedron Lett.* **1991**, *32*, 1055–1058.
- (12) For review, see: McGarrigle, E. M.; Gilheany, D. G. *Chem. Rev.* **2005**, *105*, 1563–1602.
- (13) (a) Houk, K. N.; DeMello, N. C.; Condroski, K.; Fennen, J.; Kasuga, T. *Proceedings of the ECHET96 Electronic Conference*, 1996, <http://www.ch.ia.ac.uk/ectoc/echet96>. (b) Strassner, T.; Houk, K. N. *Org. Lett.* **1999**, *1*, 419–421. (c) Linde, C.; Åkermar, B.; Norrby, P.-O.; Svensson, M. J. *Am. Chem. Soc.* **1999**, *121*, 5083–5084. (d) Jacobsen, H.; Cavallo, L. *Chem.—Eur. J.* **2001**, *7*, 800–807. (e) El-Bahraoui, J.; Wiest, O.; Feichtinger, D.; Plattner, D. A. *Angew. Chem., Int. Ed.* **2001**, *40*, 2073–2076. (f) Abashkin, Y. G.; Collins, J. R.; Burt, S. K. *Inorg. Chem.* **2001**, *40*, 4040–4048. (g) Lipkowitz, K. B.; Schefzick, S. *Chirality* **2002**, *14*, 677–682. (h) Cavallo, L.; Jacobsen, H. *J. Org. Chem.* **2003**, *68*, 6202–6207. (i) Khavrutskii, I. V.; Musaev, D. G.; Morokuma, K. *J. Am. Chem. Soc.* **2003**, *125*, 13879–13889. (j) Khavrutskii, I. V.; Musaev, D. G.; Morokuma, K. *Proc. Natl. Acad. Sci. U.S.A.* **2004**, *101*, 5743–5748.
- (14) (a) Feichtinger, D.; Plattner, D. A. *Angew. Chem., Int. Ed. Engl.* **1997**, *36*, 1718–1719. (b) Plattner, D. A.; Feichtinger, D.; El-Bahraoui, J.; Wiest, O. *Int. J. Mass Spectrom.* **2000**, *195/196*, 351–362. (c) Feichtinger, D.; Plattner, D. A. *J. Chem. Soc., Perkin Trans. 2* **2000**, 1023–1028. (d) Feichtinger, D.; Plattner, D. A. *Chem.—Eur. J.* **2001**, *7*, 591–599.
- (15) (a) Sabater, M. J.; Alvaro, M.; García, H.; Palomares, E.; Scaiano, J. C. *J. Am. Chem. Soc.* **2001**, *123*, 7074–7080. (b) Liu, S.-Y.; Soper, J. D.; Yang, J. Y.; Rybak-Akimova, E. V.; Nocera, D. G. *Inorg. Chem.* **2006**, *45*, 7572–7574.
- (16) (a) Bryliakov, K. P.; Babushkin, D. E.; Talsi, E. P. *J. Mol. Catal. A* **2000**, *158*, 19–35. (b) Adam, W.; Mock-Knoblach, C.; Saha-Möller, C. R.; Herderich, M. J. *Am. Chem. Soc.* **2000**, *122*, 9685–9691. (c) Campbell, K. A.; Lashley, M. R.; Wyatt, J. K.; Nantz, M. H.; Britt, R. D. *J. Am. Chem. Soc.* **2001**, *123*, 5710–5719. (d) Feth, M. P.; Bolm, C.; Hildebrand, J. P.; Köhler, M.; Beckmann, O.; Bauer, M.; Ramamonjisoa, R.; Bertagnolli, H. *Chem.—Eur. J.* **2003**, *9*, 1348–1359.
- (17) Kurahashi, T.; Kikuchi, A.; Tosha, T.; Shiro, Y.; Kitagawa, T.; Fujii, H. *Inorg. Chem.* **2008**, *47*, 1674–1686.

- (18) Green, M. T.; Dawson, J. H.; Gray, H. B. *Science* **2004**, *304*, 1653–1656.
- (19) (a) Yin, G.; Danby, A. M.; Kitko, D.; Carter, J. D.; Scheper, W. M.; Busch, D. H. *J. Am. Chem. Soc.* **2007**, *129*, 1512–1513. (b) Yin, G.; Danby, A. M.; Kitko, D.; Carter, J. D.; Scheper, W. M.; Busch, D. H. *J. Am. Chem. Soc.* **2008**, *130*, 16245–16253.
- (20) (a) Bordwell, F. G.; Cheng, J.-P.; Harrelson, J. A., Jr. *J. Am. Chem. Soc.* **1988**, *110*, 1512–1513. (b) Bordwell, F. G.; Cheng, J.-P.; Ji, G.-Z.; Satish, A. V.; Zhang, X. J. *Am. Chem. Soc.* **1991**, *113*, 9790–9795.
- (21) (a) Mayer, J. M. *Acc. Chem. Res.* **1998**, *31*, 441–450. (b) Mayer, J. M. *Annu. Rev. Phys. Chem.* **2004**, *55*, 363–390.
- (22) Palucki, M.; Pospisil, P. J.; Zhang, W.; Jacobsen, E. N. *J. Am. Chem. Soc.* **1994**, *116*, 9333–9334.
- (23) (a) Zdilla, M. J.; Dexheimer, J. L.; Abu-Omar, M. M. *J. Am. Chem. Soc.* **2007**, *129*, 11505–11511. (b) Sastri, C. V.; Lee, J.; Oh, K.; Lee, Y. J.; Lee, J.; Jackson, T. A.; Ray, K.; Hirao, H.; Shin, W.; Halfen, J. A.; Kim, J.; Que, L., Jr.; Shaik, S.; Nam, W. *Proc. Natl. Acad. Sci. U.S.A.* **2007**, *49*, 19181–19186. (c) Miyazaki, S.; Kojima, T.; Mayer, J. M.; Fukuzumi, S. *J. Am. Chem. Soc.* **2009**, *131*, 11615–11624.

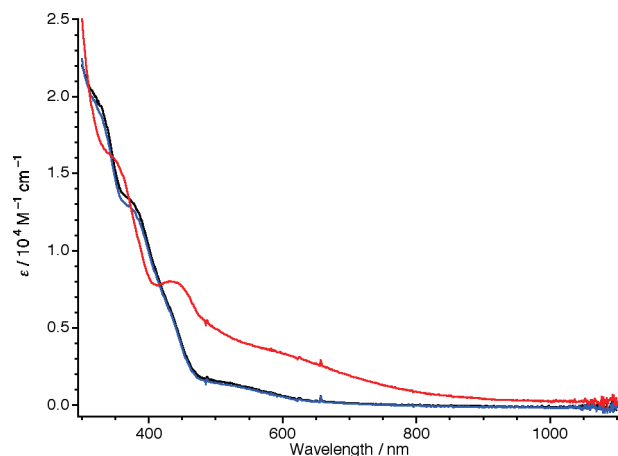


Figure 1. UV-vis spectra of a 1 mM solution of **1** (black line), **1** + 1.0 equiv of *m*-CPBA (blue line), and **1** + 1.0 equiv of *m*-CPBA + 1.0 equiv of Bu₄NOH (red line) in CH₂Cl₂ at 203 K.

be considerably different. We also carried out a quantum chemical calculation for Mn^{IV}(salen)(O) and its protonated species such as Mn^{IV}(salen)(OH).

Results and Discussion

Reaction of a Sterically Hindered **1 with *m*-CPBA.** The reaction of **1** with *m*-CPBA in the absence of a substrate is investigated under the low-temperature conditions employed for the Mn^{III}(salen)-catalyzed epoxidation using *m*-CPBA.²² As shown in Figure 1, upon the addition of 1.0 equiv of *m*-CPBA to the CH₂Cl₂ solution of **1** (depicted as a black line) at 203 K, the resulting solution shows an UV-vis spectrum almost identical with that of the starting **1** (depicted as a blue line). However, the subsequent addition of 1.0 equiv of Bu₄NOH immediately generates a distinct species with absorption maxima around 350, 435, and 600 nm (depicted as a red line). The absorption spectral features are similar to that of Mn^{IV}(salen)(O), which was identified in our previous study.¹⁷ Interestingly, when the addition sequence of *m*-CPBA and Bu₄NOH is altered, this species is not generated, suggesting that Bu₄NOH might function as a base to remove a proton from *m*-CPBA rather than as a trans axial ligand to activate *m*-CPBA. In the case of the low-temperature Mn^{III}(salen)-catalyzed epoxidation using *m*-CPBA as an oxidant,²² the use of excess *N*-methylmorpholine *N*-oxide (NMO) as an additive is reported to be critical. Then, the use of NMO instead of Bu₄NOH is also examined for the reaction of **1** with *m*-CPBA. The addition of 1.0 equiv of NMO results in exactly the same spectral change, suggesting that both NMO and Bu₄NOH might function in a similar manner upon activation of *m*-CPBA at 203 K.

Parallel-mode EPR spectroscopy of **1** shows a signal at $g = 8.1$, which displays a six-line hyperfine splitting with $A = 38$ G, as expected for the $I = 5/2$ ⁵⁵Mn nucleus (Figure 2). This signal was assigned as the transition between the $M_s = \pm 2$ level of an $S = 2$ spin system of a d⁴ Mn^{III} system.^{16c} Upon the addition of 1.0 equiv of *m*-CPBA at 203 K, the signal at $g = 8.1$ is not changed, indicating that the Mn^{III} center remains intact. Upon the subsequent addition of 1.0 equiv of Bu₄NOH, perpendicular-mode EPR spectroscopy detects signals at $g = 5.0$, 3.1, and 1.9, which coincide with the disappearance of a parallel-mode EPR

signal at $g = 8.1$ from **1**. The signals at $g = 5.0$, 3.1, and 1.9, which are derived from an $S = 3/2$ spin system of a d³ Mn^{IV} system,^{16c} are almost as intense as those of authentic Mn^{IV}(salen)(O) and Mn^{IV}(salen)(OH), which were prepared by alternative methods,¹⁷ as shown in Figure S1 (Supporting Information). Thus, this solution contains Mn^{IV} species exclusively. Comparison of the EPR spectra (Figure S1 in the Supporting Information) suggests that the resulting solution may contain not only Mn^{IV}(salen)(O) but also Mn^{IV}(salen)(OH).

Then, the solution generated by the addition of 1.0 equiv of *m*-CPBA and Bu₄NOH to **1** at 203 K was investigated by XAS. An XAS measurement was carried out in propionitrile, in which the reaction of **1** with 1.0 equiv of *m*-CPBA and Bu₄NOH generates the same intermediate, as confirmed by UV-vis and EPR. As seen from the Mn K-edge X-ray absorption near-edge structure (XANES) regions (Figure 3a), the preedge height is not increased before and after the addition of *m*-CPBA and Bu₄NOH, which is also the case for Mn^{IV}(salen)(OH) and Mn^{IV}(salen)(O).¹⁷ Both the preedge and the absorption edge are shifted to higher energies by 0.1 and 0.7 eV upon the addition of *m*-CPBA and Bu₄NOH. This shift may correspond to the change in the oxidation state from Mn^{III} to Mn^{IV}. The extended X-ray absorption fine structure (EXAFS) spectrum of the solution in Figure 3b shows a peak at a phase-shifted distance $R' \approx 1$ Å. This peak corresponds to the Mn^{IV}=O bond (1.58 Å), in comparison with our previous EXAFS analysis of Mn^{IV}(salen)(O).¹⁷ However, the intensity of this peak is somewhat lower than that in authentic Mn^{IV}(salen)(O).

This is consistent with the EPR observation that the solution may contain Mn^{IV}(salen)(O) as well as Mn^{IV}(salen)(OH), which has a longer Mn^{IV}–O bond (1.83 Å), as determined by our previous EXAFS analysis.¹⁷ Table 1 shows one of the possible curve-fitting simulations in which both coordination numbers and interatomic distances are allowed to vary. The simulation suggests that the solution may contain 70% Mn^{IV}(salen)(O) (shells 1–3) and 30% Mn^{IV}(salen)(OH) (shells 2 and 3). Scheme 1 summarizes Mn^{IV}(salen) species to be formed under certain conditions.¹⁷

Quantum Chemical Study of Mn^{IV}(salen)(O), Mn^{IV}(salen)(OH), and Mn^{III}(salen⁺)(OH₂). In order to provide a theoretical support for the experimental observation, we carried out a quantum chemical calculation, using virtually the same Mn^{III}(salen) model with **1** as shown in Figure 4. Figure 4 also shows an optimized structure for Mn^{IV}(salen)(O). Figure 5 illustrates the difference in coordination geometries for Mn^{IV}(salen)(O) and its protonation products. An optimized geometry for Mn^{IV}(salen)(O) in Table 2 shows a Mn–O3 bond distance of 1.642 Å, which is a little bit longer but is in qualitative agreement with the experimental distance of 1.58 Å derived from the previous EXAFS analysis.¹⁷ Protonation of Mn^{IV}(salen)(O) to Mn^{IV}(salen)(OH) prolongs a Mn–O3 bond distance to 1.797 Å, which is also consistent with the EXAFS distance of 1.83 Å.¹⁷ Upon further protonation of Mn^{IV}(salen)(OH), the Mn–O3 bond distance is significantly prolonged to 2.258 Å. Ghosh and Gonzalez reported theoretical studies on high-valent manganese porphyrins, in which Mn^{IV}=O bond distances in [Mn^{IV}(porphyrin)(O)(PF₆)][−], Mn^{IV}(porphyrin)(O)(pyridine), and [Mn^{IV}(porphyrin)(O)(F)][−] are calculated to be

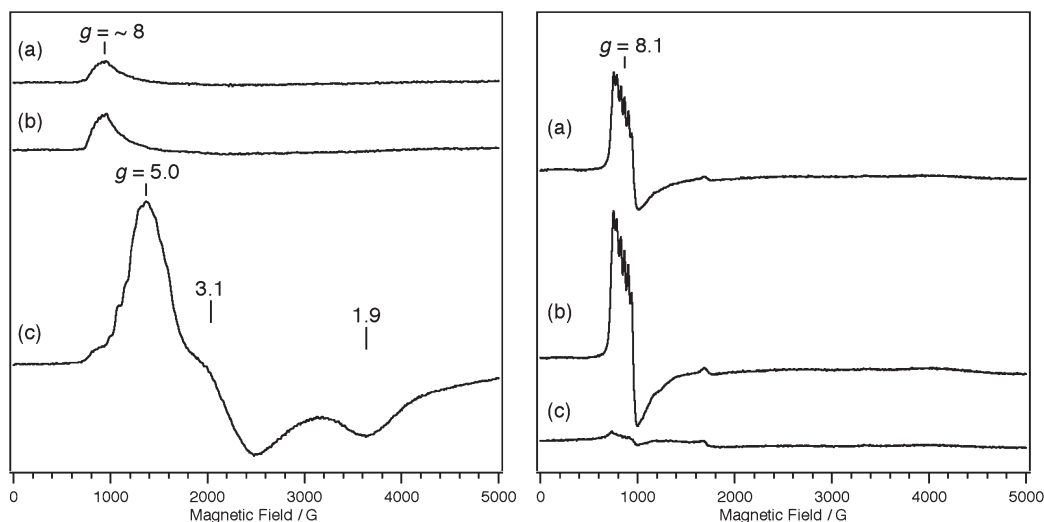


Figure 2. X-band EPR spectra of (a) **1**, (b) **1** + 1.0 equiv of *m*-CPBA, and (c) **1** + 1.0 equiv of *m*-CPBA + 1.0 equiv of Bu₄NOH: (left) perpendicular mode; (right) parallel mode. Conditions: temperature, 5 K; solvent, frozen CH₂Cl₂ containing 0.1 M Bu₄NClO₄; microwave frequency, 9.69 (perpendicular) or 9.53 (parallel) GHz; microwave power, 2.000 mW; modulation amplitude, 10 G; modulation frequency, 100 kHz; time constant, 81.92 ms; conversion time, 81.92 ms.

1.668, 1.674, and 1.709 Å, respectively.²⁴ The Mn^{IV}=O bond distance in the present case is shorter than those, possibly because of the absence of a sixth coordination ligand trans to the oxo ligand. Borovik and co-workers reported a monomeric Mn^{IV}=O complex, in which the Mn^{IV}=O moiety is stabilized by three hydrogen bonds from amides.^{8a} Their density functional theory (DFT) calculations showed that hydrogen bonding prolongs the Mn^{IV}=O bond distance to 1.706 Å, which is longer than that in Mn^{IV}-(salen)(O) but is shorter than that in Mn^{IV}-(salen)(OH).

As shown in Table 3, electronic structures of Mn^{IV}-(salen)(O) and Mn^{IV}-(salen)(OH) are best described as high-spin d³ Mn^{IV} with an electronic configuration of (d_{xy})¹(d_{yz})¹(d_{nb})¹, which accounts for $S = 3/2$ EPR signals for Mn^{IV}-(salen)(O) and Mn^{IV}-(salen)(OH).¹⁷ In the case of Mn^{IV}-(salen)(O), a substantial spin population is found on the O3 ligand, while spin populations on the d_{xy} orbitals are decreased as compared with those of Mn^{IV}-(salen)(OH). This is indicative of a Mn(d_{xy})-to-O3 spin delocalization, which means a π -bonding character for Mn–O3 in Mn^{IV}-(salen)(O). Protonation of Mn^{IV}-(salen)(O) prolongs a Mn–O3 bond distance as compared with Mn^{IV}-(salen)(O), leading to an increased spin population on the d_{xy} orbital due to a stabilization of this orbital. Protonation of Mn^{IV}-(salen)(OH) increases a spin population on the d_{xy} orbital more significantly because of a much longer Mn–O3 bond distance. It is interesting to note that a spin population with a negative sign is remarkably increased on the salen ligand upon protonation of Mn^{IV}-(salen)(OH). This indicates a salen ligand radical antiferromagnetically coupled to the high-spin d⁴ Mn^{III}, which is nicely consistent with our previous spectroscopic assignment as Mn^{III}(salen^{•+})(OH₂) of an $S_t = 3/2$ spin system.¹⁷ The present theoretical calculation as well as the previous experiment indicates conversion from manganese(IV) phenolate in Mn^{IV}-(salen)(OH) to a manganese(III) phenoxyl radical in Mn^{III}(salen^{•+})(OH₂), because protonation of hydroxo on manganese significantly stabilizes the d_{xy} orbital

relative to the π orbital of the salen ligand, leading to intramolecular electron transfer from the salen ligand to the Mn^{IV} center. Quantum chemical calculations suggest a lesser degree of a similar salen ligand radical also for Mn^{IV}-(salen)(OH), but a possible contribution of Mn^{III}-(salen^{•+})(OH) was not evident in the previous experiment.¹⁷ Ni(salen) has recently attracted considerable attention because a one-electron-oxidized form of Ni^{II}(salen) exhibits valence tautomerism between Ni^{III}(salen) and Ni^{II}-(salen^{•+}).²⁵ In the case of Ni^{II}(salen^{•+}), DFT calculations showed that ca. 80% of the unpaired spin is located on the salen ligand.^{25b,e,f} A similar equilibrium between the high-valent metal species and the ligand-radical species was also proposed for a one-electron-oxidized form of Cu^{II}(salen).²⁶

Reactions of Mn^{IV}-(salen)(O) and Mn^{IV}-(salen)(OH) with Substituted Phenols. We investigate the reactivity of the Mn^{IV}-(salen) mixture, which is shown to contain Mn^{IV}-(salen)(O) and Mn^{IV}-(salen)(OH) as above. The Mn^{IV}-(salen) mixture is prepared under the conditions (1 mM) shown in Figure 1, and the solution of 2,6-di-*tert*-butylphenol (10 mM) is added under pseudo-first-order conditions at 203 K. The Mn^{IV}-(salen) mixture is reduced to Mn^{III}(salen) within seconds, and this reaction is too fast to follow with an UV–vis spectrometer. To follow the reaction process by Mn^{IV}-(salen)(O) and Mn^{IV}-(salen)(OH) in

(25) (a) Shimazaki, Y.; Tani, F.; Fukui, K.; Naruta, Y.; Yamauchi, O. *J. Am. Chem. Soc.* **2003**, *125*, 10512–10513. (b) Rothaus, O.; Jarjayes, O.; Thomas, F.; Philouze, C.; Perez Del Valle, C.; Saint-Aman, E.; Pierre, J.-L. *Chem.—Eur. J.* **2006**, *12*, 2293–2302. (c) Rothaus, O.; Thomas, F.; Jarjayes, O.; Philouze, C.; Saint-Aman, E.; Pierre, J.-L. *Chem.—Eur. J.* **2006**, *12*, 6953–6962. (d) Shimazaki, Y.; Yajima, T.; Tani, F.; Karasawa, S.; Fukui, K.; Naruta, Y.; Yamauchi, O. *J. Am. Chem. Soc.* **2007**, *129*, 2559–2568. (e) Benisvy, L.; Kannappan, R.; Song, Y.-F.; Milikisyants, S.; Huber, M.; Mutikainen, I.; Turpeinen, U.; Gamez, P.; Bernasconi, L.; Baerends, E. J.; Hartl, F.; Reedijk, J. *Eur. J. Inorg. Chem.* **2007**, 637–642. (f) Rothaus, O.; Jarjayes, O.; Perez Del Valle, C.; Philouze, C.; Thomas, F. *Chem. Commun.* **2007**, 4462–4464. (g) Storr, T.; Wasinger, E. C.; Pratt, R. C.; Stack, T. D. P. *Angew. Chem., Int. Ed.* **2007**, *46*, 5198–5201. (h) Shimazaki, Y.; Stack, T. D. P.; Storr, T. *Inorg. Chem.* **2009**, *48*, 8383–8392.

(26) Storr, T.; Verma, P.; Pratt, R. C.; Wasinger, E. C.; Shimazaki, Y.; Stack, T. D. P. *J. Am. Chem. Soc.* **2008**, *130*, 15448–15459.

(24) Ghosh, A.; Gonzalez, E. *Isr. J. Chem.* **2000**, *40*, 1–8.

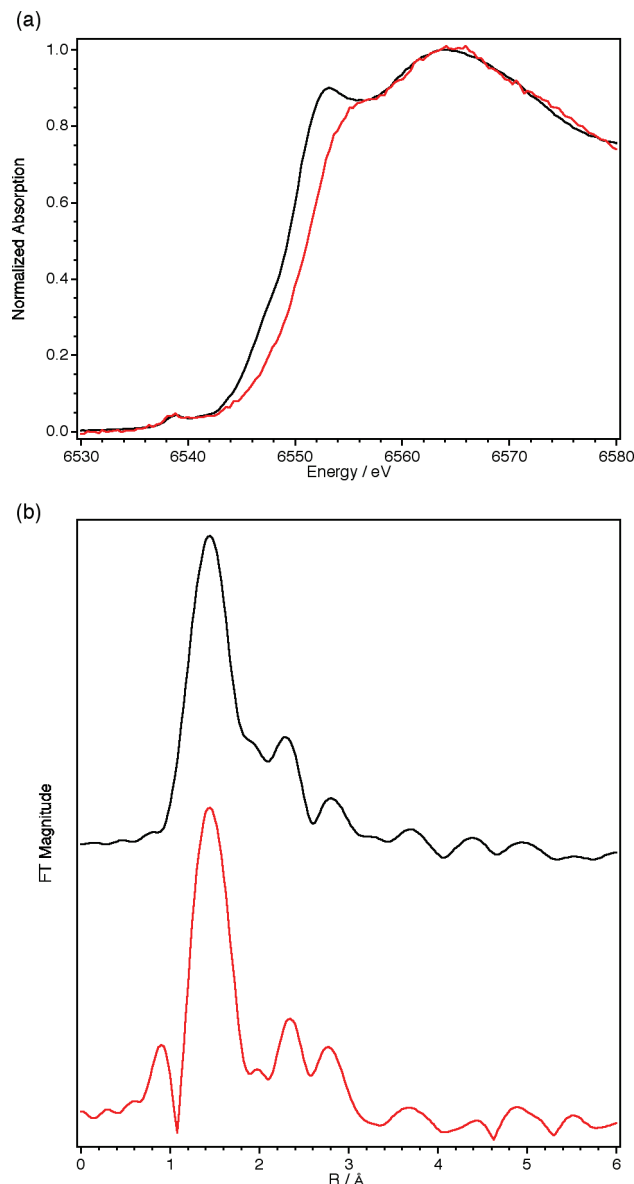


Figure 3. (a) XANES spectra of **1** (black line) and the solution of **1** + 1.0 equiv of *m*-CPBA + 1.0 equiv of Bu₄NOH (red line). (b) Fourier transforms of the EXAFS data for **1** (black line) and the solution of **1** + 1.0 equiv of *m*-CPBA + 1.0 equiv of Bu₄NOH (red line). XAS data were measured for **1** in the solid state at room temperature and for the 20 mM solution of **1** + 1.0 equiv of *m*-CPBA + 1.0 equiv of Bu₄NOH in frozen propionitrile at 10 K.

Table 1. EXAFS Analysis of the Solution of **1** + 1.0 equiv of *m*-CPBA + 1.0 equiv of Bu₄NOH^a

shell	<i>N</i> ^b	<i>R</i> (Å) ^c	σ^2 (Å ²) ^d	ΔE_0 (eV) ^e
1	0.68	1.570	0.003	13.22
2	2.32	1.796	0.009	4.16
3	2.00	1.954	0.003	-5.09

^a *R* factor, defined as $\sum |y_{\text{exp}}(i) - y_{\text{theo}}(i)| / \sum |y_{\text{exp}}(i)|$, where y_{exp} and y_{theo} are experimental and theoretical data points, respectively, equal to 7.67%. The curve-fitting results are shown in Figure S2 (Supporting Information). ^b The total coordination number was fixed at 3 for the sum of the shells 1 and 2. The coordination number was fixed at 2 for shell 3. ^c Interatomic distances estimated from the EXAFS curve fitting. ^d Debye–Waller factor. ^e Shift in photoelectron energy zero.

more detail, we attempted to prepare the Mn^{IV}(salen) mixture at lower concentration. However, the Mn^{IV}(salen)

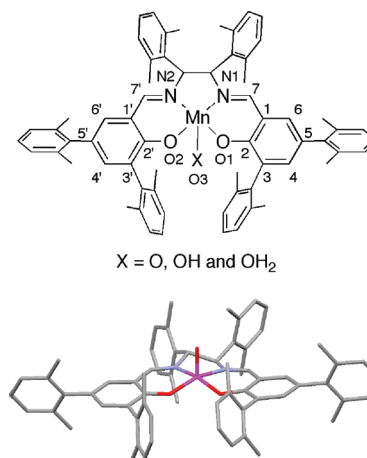


Figure 4. Mn(salen) for quantum chemical calculations and the optimized structure for Mn^{IV}(salen)(O).

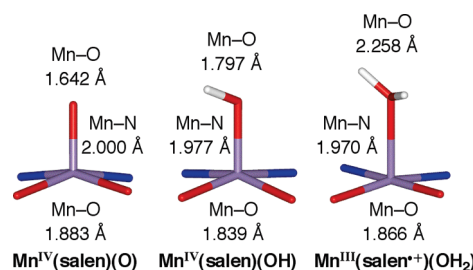
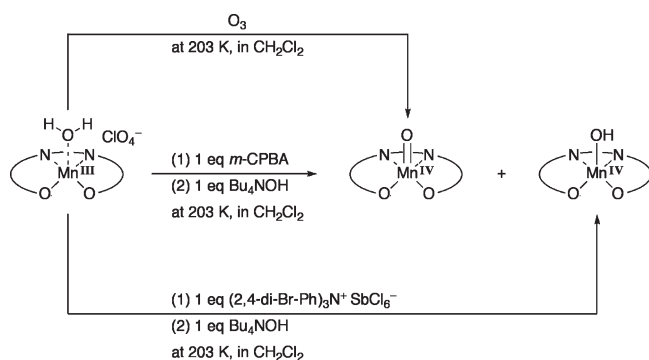


Figure 5. Calculated coordination geometries for Mn^{IV}(salen)(O), Mn^{IV}(salen)(OH), and Mn^{III}(salen⁺⁺)(OH₂).

Scheme 1. Mn^{IV}(salen) Species to be Formed under Certain Conditions



mixture could not be formed under the low-concentration conditions possibly because the bimolecular reaction of **1** with *m*-CPBA is slow. Moreover, we attempted to carefully dilute a 1 mM solution of the Mn^{IV}(salen) mixture by adding CH₂Cl₂ at 203 K, but this was not successful because of decomposition.

Alternatively, Mn^{IV}(salen)(O) is prepared by the reaction of **1** with O₃, and Mn^{IV}(salen)(OH) is prepared by one-electron oxidation of **1** and a subsequent ligand exchange with OH, as described previously.¹⁷ Both species are successfully prepared under conditions (0.05 mM) that are appropriate for a kinetic study with substituted phenols at 203 K. As shown in Figure 6, upon the addition of 2,6-di-*tert*-butylphenol, the UV–vis spectrum of Mn^{IV}(salen)(O) (depicted as a red line) is changed with clear isosbestic points, and the decay of absorption at 600 nm

Table 2. Selected Optimized Geometrical Parameters and Relative Energies

	Mn ^{IV} (salen)-(O)	Mn ^{IV} (salen)-(OH)	Mn ^{III} (salen ⁺⁺)-(OH ₂)
Mn–O3/Å	1.642	1.797	2.258
Mn–O1/Å	1.882	1.844	1.864
Mn–O2/Å	1.883	1.833	1.868
Mn–N1/Å	2.003	1.970	1.971
Mn–N2/Å	1.997	1.984	1.968
O1–C2/Å	1.307	1.318	1.315
O2–C2'/Å	1.307	1.326	1.311
N1–C7/Å	1.295	1.302	1.300
N2–C7'/Å	1.295	1.299	1.303
C1–C7/Å	1.430	1.425	1.432
C1'–C7'/Å	1.431	1.428	1.431
Mn–N ₂ O ₂ plane/Å	0.327	0.308	0.129
O1–Mn–N2/deg	161.78	159.65	174.18
O2–Mn–N1/deg	157.97	161.65	166.27
relative energies/kcal mol ^{−1}	0	−240.0	−504.0

Table 3. Gross Orbital Spin Populations^a

	Mn ^{IV} (salen)(O)	Mn ^{IV} (salen)(OH)	Mn ^{III} (salen ⁺⁺)(OH ₂)
Mn d _{σ1}	0.170	0.326	0.883
Mn d _{σ2}	0.100	0.159	0.173
Mn d _π	0.698	0.834	0.770
Mn d _π	0.663	0.843	0.916
Mn d _{nb}	0.907	0.875	0.923
total of Mn	2.562	3.087	3.859
O3	0.430	0.015	0.026
salen ligand	0.008	−0.102	−0.885

^a The d_{σ1} and d_π orbitals represent σ and π bonding to O3, and the d_{σ2} orbital represents σ bonding to the salen ligand. d_{nb} represents a non-bonding orbital.

follows pseudo-first-order kinetics under conditions of excess phenol. For data fitting, the data points within 30 s after the addition of 2,6-di-*tert*-butylphenol were excluded because the solution may not be well mixed. A reaction of Mn^{IV}(salen)(O) with 2,6-di-*tert*-butylphenol is very fast, and thus a minimum amount of phenols [10–40 equiv relative to Mn^{IV}(salen)(O)] is utilized. The pseudo-first-order rate constants (k_{obs}) vary linearly with the concentration of 2,6-di-*tert*-butylphenol (Figure S3 in the Supporting Information), yielding a second-order rate constant, $k_2 = 11.7 \text{ M}^{-1} \text{ s}^{-1}$. In a similar manner, second-order rate constants for oxidation reactions of Mn^{IV}(salen)(O) with other phenols (3',5'-di-*tert*-butyl-4'-hydroxyacetophenone and 3,5-di-*tert*-butyl-4-hydroxybenzonitrile) and 1,4-cyclohexadiene were determined (Figures S4–S6 in the Supporting Information), and the data are summarized in Table 4.

Figure 7a shows a UV–vis spectral change of Mn^{IV}(salen)(OH) in the presence of 2,6-di-*tert*-butylphenol. As indicated by the decay of absorption at 720 nm, Mn^{IV}(salen)(OH) (depicted as a red line) also reacts with 2,6-di-*tert*-butylphenol but at much slower rate as compared with Mn^{IV}(salen)(O). The reactions of Mn^{IV}(salen)(OH) with 2,6-di-*tert*-butylphenol are also carried out under conditions of a slight excess of 2,6-di-*tert*-butylphenol (10–50 equiv). The kinetic trace is comprised of two components, and we utilized the data points in the former region for estimating the k_{obs} values. In clear contrast to Mn^{IV}(salen)(O), the k_{obs} values do not show a linear correlation with the concentration of 2,6-di-*tert*-butylphenol (Figure 7b). This might be due to binding of

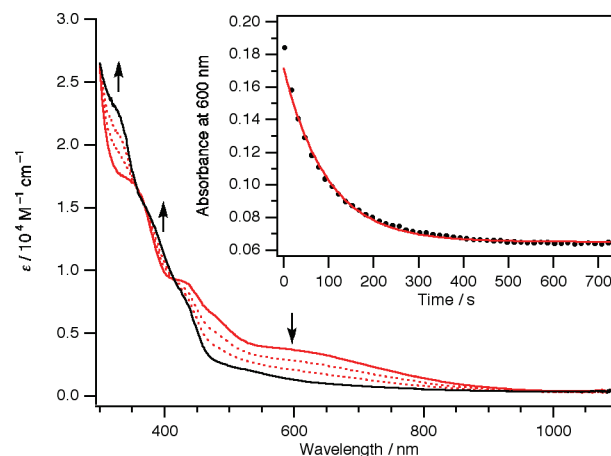


Figure 6. UV–vis spectral changes upon reaction of Mn^{IV}(salen)(O) ($5.10 \times 10^{-5} \text{ M}$) with 2,6-di-*tert*-butylphenol ($5.10 \times 10^{-4} \text{ M}$) in CH₂Cl₂ at 203 K. The spectra at 0, 30, 90, and 720 s after the addition of 2,6-di-*tert*-butylphenol are shown. Inset: Decay of the absorption at 600 nm derived from Mn^{IV}(salen)(O) ($5.10 \times 10^{-5} \text{ M}$) in the presence of 2,6-di-*tert*-butylphenol ($5.10 \times 10^{-4} \text{ M}$) in CH₂Cl₂ at 203 K.

2,6-di-*tert*-butylphenol by Mn^{IV}(salen)(OH) prior to the rate-limiting oxidation reactions (Scheme 2).

Under conditions of excess phenols, an observed rate constant, k_{obs} , is given by eq 1.

$$k_{\text{obs}} = \frac{k_1 K [\text{phenol}]}{1 + K [\text{phenol}]} \quad (1)$$

The simulation curve (red line) in Figure 7 suggests that rather strong binding of 2,6-di-*tert*-butylphenol by Mn^{IV}(salen)(OH) ($K \approx 5000 \text{ M}^{-1}$) would give observed kinetics for the reaction of Mn^{IV}(salen)(OH) with 2,6-di-*tert*-butylphenol. We hypothesize that the ability of Mn^{IV}(salen)(OH) to strongly bind a phenol might be ascribed to double hydrogen bonding as shown in Scheme 1. Reactions of Mn^{IV}(salen)(OH) with other substituted phenols (2,6-di-*tert*-butyl-4-methylphenol, 2,4,6-tri-*tert*-butylphenol, and 3',5'-di-*tert*-butyl-4'-hydroxyacetophenone) are also carried out (Figures S7–S9 in the Supporting Information), and the averaged k_{obs} values, which are independent of the concentration of phenols, are listed in Table 4. A reaction of Mn^{IV}(salen)(OH) with 3,5-di-*tert*-butyl-4-hydroxybenzonitrile is negligibly slow under identical conditions. However, the use of a large excess of 3,5-di-*tert*-butyl-4-hydroxybenzonitrile [200 equiv relative to Mn^{IV}(salen)(OH)] generates a stable Mn^{IV} species with the absorption maximum shifted from 720 nm to shorter wavelength, which precludes the precise determination of the k_{obs} value.

Reactions of Mn^{IV}(salen)(O) and Mn^{IV}(salen)(OH) with 2,6-di-*tert*-butylphenol were monitored by perpendicular- and parallel-mode EPR spectroscopy. Upon reactions of Mn^{IV}(salen)(O) and Mn^{IV}(salen)(OH) with 2,6-di-*tert*-butylphenol at 203 K for 2 h, EPR signals from Mn^{IV} species in a perpendicular mode disappear, while parallel-mode EPR spectroscopy shows regeneration of the signals at $g = 8.1$ from Mn^{III} species, which are almost as intense as that from the starting **1** (Figures S10 and S11 in the Supporting Information). It is thus indicated that both Mn^{IV}(salen)(O) and Mn^{IV}(salen)(OH) are reduced mainly to Mn^{III}(salen) upon reactions with 2,6-di-*tert*-butylphenol. Perpendicular-mode EPR spectroscopy

Table 4. Rate Constants for Hydrogen-Atom Abstraction by $\text{Mn}^{\text{IV}}(\text{salen})(\text{O})$ and $\text{Mn}^{\text{IV}}(\text{salen})(\text{OH})$ in CH_2Cl_2 at 203 K^a

	$\text{Mn}^{\text{IV}}(\text{salen})(\text{O})$ $k_2^b/\text{M}^{-1} \text{s}^{-1}$	$\text{Mn}^{\text{IV}}(\text{salen})(\text{OH})$ $k_{\text{obs}}^c/\text{s}^{-1}$
1,4-cyclohexadiene	$2.3 \times 10^{-2} \pm 0.005$	$\approx 0^e$
4-Me-2,6- <i>tert</i> -Bu ₂ C ₆ H ₂ OH	$>100^d$	$2.1 \times 10^{-2} \pm 4.0 \times 10^{-4}$
2,4,6- <i>tert</i> -Bu ₃ C ₆ H ₂ OH	$>100^d$	$6.8 \times 10^{-3} \pm 1.0 \times 10^{-4}$
2,4- <i>tert</i> -Bu ₂ C ₆ H ₃ OH	$>100^d$	$>1.0 \times 10^{-1}$ ^d
2,6- <i>tert</i> -Bu ₂ C ₆ H ₃ OH	11.7 ± 2.1 ($k_{\text{H}}/k_{\text{D}}$ 5.3)	$1.9 \times 10^{-3} \pm 1.1 \times 10^{-4}$ ($k_{\text{H}}/k_{\text{D}}$ = 9.5)
4-CH ₃ CO-2,6- <i>tert</i> -Bu ₂ C ₆ H ₂ OH	2.1 ± 0.5	$2.3 \times 10^{-4} \pm 1.1 \times 10^{-4}$
4-NC-2,6- <i>tert</i> -Bu ₂ C ₆ H ₂ OH	1.7 ± 0.2	$\approx 0^e$

^a Reaction conditions: $[\text{Mn}^{\text{IV}}(\text{salen})(\text{O})]$ or $[\text{Mn}^{\text{IV}}(\text{salen})(\text{OH})] = 5.10 \times 10^{-5} \text{ M}$, $[\text{substrate}] = 5.0 \times 10^{-4}$ – $2.5 \times 10^{-3} \text{ M}$. ^b Second-order rate constants. ^c Averaged pseudo-first-order rate constants, which are not dependent on the concentration of substituted phenols. ^d $\text{Mn}^{\text{IV}}(\text{salen})(\text{O})$ or $\text{Mn}^{\text{IV}}(\text{salen})(\text{OH})$ are reduced within 20 s under the reaction conditions at 203 K, and thus the rate constants could not be determined precisely. ^e UV–vis spectral changes of $\text{Mn}^{\text{IV}}(\text{salen})(\text{OH})$ ($5.10 \times 10^{-5} \text{ M}$) in the presence of the substrate ($1.0 \times 10^{-2} \text{ M}$) are negligibly small.

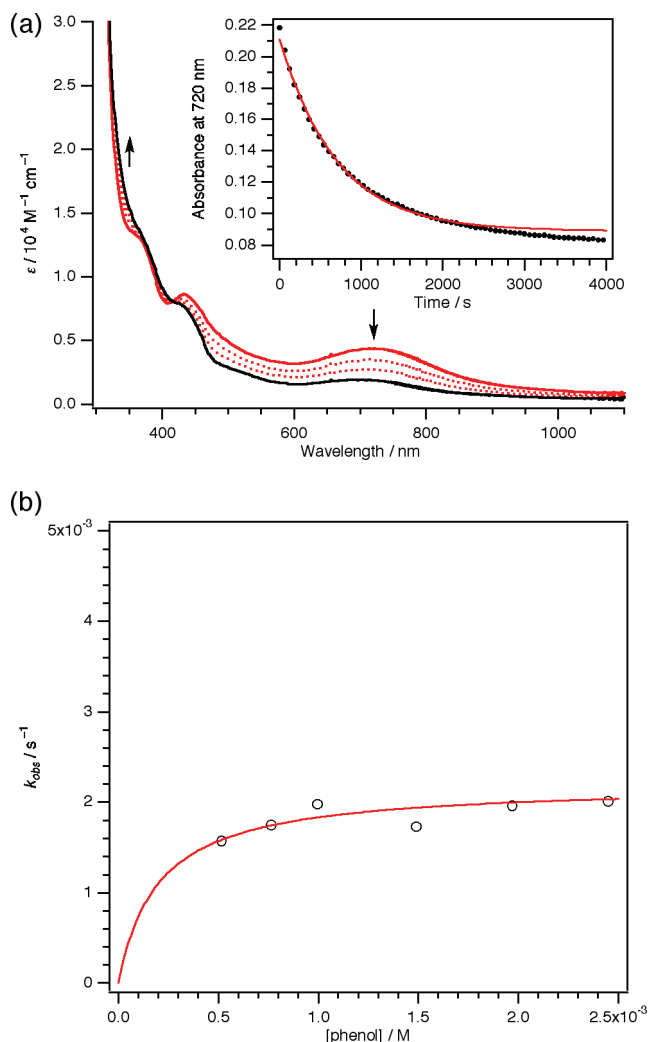


Figure 7. (a) UV–vis spectral changes upon the reaction of $\text{Mn}^{\text{IV}}(\text{salen})(\text{OH})$ ($5.10 \times 10^{-5} \text{ M}$) with 2,6-di-*tert*-butylphenol ($1.49 \times 10^{-3} \text{ M}$) in CH_2Cl_2 at 203 K. The spectra at 0, 240, 660, and 2100 s after the addition of 2,6-di-*tert*-butylphenol are shown. Inset: Decay of absorption at 720 nm derived from $\text{Mn}^{\text{IV}}(\text{salen})(\text{OH})$ ($5.10 \times 10^{-5} \text{ M}$) in the presence of 2,6-di-*tert*-butylphenol ($1.49 \times 10^{-3} \text{ M}$) in CH_2Cl_2 at 203 K. (b) Plot of the pseudo-first-order rate constant (k_{obs}) vs concentration of 2,6-di-*tert*-butylphenol ($[\text{phenol}]$). Data are designated by points; the simulation curve is designated by a red line, $K = 5000 \text{ M}^{-1}$ and $k_1 = 2.2 \times 10^{-3} \text{ s}^{-1}$ (eq 1).

detected an additional intense signal at $g = 2.0$ in the case of $\text{Mn}^{\text{IV}}(\text{salen})(\text{O})$ and a weak signal at $g = 2.0$ with a six-line hyperfine splitting in the case of $\text{Mn}^{\text{IV}}(\text{salen})(\text{OH})$ after the reaction with 2,6-di-*tert*-butylphenol. These additional signals were not characterized. In the case of

2,4,6-tri-*tert*-butylphenol as a substrate, a sharp signal at $g = 2.0$ was observed, indicative of the formation of a phenoxyl radical from 2,4,6-tri-*tert*-butylphenol (Figure S12 in the Supporting Information).

As shown in Table 4, the oxidation of OH bonds in substituted phenols by $\text{Mn}^{\text{IV}}(\text{salen})(\text{O})$ proceeds orders of magnitude faster than the oxidation of CH bonds in 1,4-cyclohexadiene, although BDE_{OH} (OH bond dissociation enthalpy) values of substituted phenols (81.0–84.2 kcal mol^{−1})²⁷ are even higher than the BDE_{CH} (CH bond dissociation enthalpy) values of 1,4-cyclohexadiene (76.0 kcal mol^{−1}).²⁸ Such marked variations in rates between different classes of substrates (O–H vs C–H) of similar bond strengths have already been addressed in detail in other systems.²⁹ $\text{Mn}^{\text{IV}}(\text{salen})(\text{O})$ readily reacts with 3,5-di-*tert*-butyl-4-hydroxybenzonitrile ($\text{BDE}_{\text{OH}} = 84.2 \text{ kcal mol}^{-1}$), while $\text{Mn}^{\text{IV}}(\text{salen})(\text{OH})$ reacts with 3',5'-di-*tert*-butyl-4'-hydroxyacetophenone ($\text{BDE}_{\text{OH}} = 83.1 \text{ kcal mol}^{-1}$) much more slowly under identical conditions than $\text{Mn}^{\text{IV}}(\text{salen})(\text{O})$ and does not react with 3,5-di-*tert*-butyl-4-hydroxybenzonitrile. It is thus indicated that the thermodynamic hydrogen-atom-abstracting ability of $\text{Mn}^{\text{IV}}(\text{salen})(\text{OH})$ is about 83 kcal mol^{−1}, but the thermodynamic hydrogen-atom-abstracting ability of $\text{Mn}^{\text{IV}}(\text{salen})(\text{O})$ well exceeds 84 kcal mol^{−1}. The $\text{Mn}^{\text{IV}}=\text{O}$ unit shows higher reactivity than the $\text{Mn}^{\text{IV}}\text{OH}$ unit in the anionic salen platform, which is also the case for Busch's neutral macrocyclic ligand.¹⁹

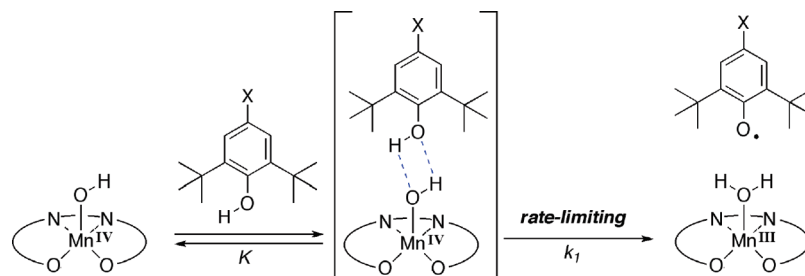
A significant kinetic isotope effect ($k_{\text{H}}/k_{\text{D}} = 5.3$ and 9.5, respectively) was observed for reactions of $\text{Mn}^{\text{IV}}(\text{salen})(\text{O})$ and $\text{Mn}^{\text{IV}}(\text{salen})(\text{OH})$ with 2,6-di-*tert*-butylphenol-*d* (~90% deuteration) in D_2O -pre-equilibrated CH_2Cl_2 ³⁰ (Figures S14 and S15 in the Supporting Information).

(27) BDE_{OH} values of substituted phenols are adopted from the following references. See also ref 23a. (a) Lucarini, M.; Pedrielli, P.; Pedulli, G. F.; Cabiddu, S.; Fattouni, C. *J. Org. Chem.* **1996**, *61*, 9259–9263. (b) Bordwell, F. G.; Cheng, J.-P. *J. Am. Chem. Soc.* **1991**, *113*, 1736–1743.

(28) BDE_{CH} values are adopted from the recommended data in a compilation by Luo: Luo, Y.-R. *Handbook of Bond Dissociation Energies in Organic Compounds*; CRC Press: Boca Raton, FL, 2003.

(29) Roth, J. P.; Yoder, J. C.; Won, T.-J.; Mayer, J. M. *Science* **2001**, *294*, 2524–2526.

(30) Reactions of $\text{Mn}^{\text{IV}}(\text{salen})(\text{O})$ and $\text{Mn}^{\text{IV}}(\text{salen})(\text{OH})$ with 2,6-di-*tert*-butylphenol-*d* were carried out in a CH_2Cl_2 solvent that was washed with D_2O and then dried over 4A molecular sieves because the deuterium atom in 2,6-di-*tert*-butylphenol-*d* is readily exchanged with the hydrogen atom in residual H_2O in CH_2Cl_2 . To evaluate the loss of the deuterium atom in a nonpolar chlorinated solvent by ¹H NMR, 2,6-di-*tert*-butylphenol-*d* was dissolved in a CDCl_3 solvent that is washed with H_2O or D_2O and then dried over 4A molecular sieves (Figure S13 in the Supporting Information). Although the CDCl_3 solvent is dry enough to be a clear solution even at 203 K, the degree of deuteration is significantly lower in H_2O -pre-equilibrated CDCl_3 (~70%) than in D_2O -pre-equilibrated CDCl_3 (~90%).

Scheme 2. Possible Reaction Pathway for the Oxidation of Phenols by $\text{Mn}^{\text{IV}}(\text{salen})(\text{OH})$ 

The present $k_{\text{H}}/k_{\text{D}}$ values are larger than the kinetic deuterium isotope effects reported for the oxidation of phenols by dicopper–dioxygen complexes via a proton-coupled electron-transfer mechanism ($k_{\text{H}}/k_{\text{D}} = 1.2\text{--}1.6$)³¹ but is comparable with the kinetic deuterium isotope effects reported for the oxidation of toluene and dihydroanthracene by permanganate via a hydrogen-atom-transfer mechanism ($k_{\text{H}}/k_{\text{D}} = 6$ and 3).^{32,33} It is also shown that both $\text{Mn}^{\text{IV}}(\text{salen})(\text{O})$ and $\text{Mn}^{\text{IV}}(\text{salen})(\text{OH})$ oxidize 2,6-di-*tert*-butylphenol significantly more slowly than 2,4-di-*tert*-butylphenol, which has similar OH bond strength but has less steric demand around OH. These results indicate that the rate-determining step involves O–H bond cleavage in both cases.

Conclusion

We herein investigate a reaction of $\text{Mn}^{\text{III}}(\text{salen})$ with *m*-CPBA under low-temperature conditions, which is shown to generate $\text{Mn}^{\text{IV}}(\text{salen})(\text{O})$ as a major product and $\text{Mn}^{\text{IV}}(\text{salen})(\text{OH})$ as a minor product, instead of $\text{Mn}^{\text{V}}(\text{salen})(\text{O})$. $\text{Mn}^{\text{IV}}(\text{salen})(\text{O})$ shows a distinctively high hydrogen-atom-abstracting ability, as compared to $\text{Mn}^{\text{IV}}(\text{salen})(\text{OH})$. This might be indicative of an important role of $\text{Mn}^{\text{IV}}(\text{salen})(\text{O})$ in catalytic oxidation reactions under low-temperature conditions.

Experimental Section

Instrumentation. UV–vis spectra were recorded in a quartz cell ($l = 0.1$ or 1 cm) on an Agilent 8453 (Agilent Technologies) equipped with an USP-203 low-temperature chamber (UNISOKU). EPR spectra were recorded in a quartz cell ($d = 4$ mm) at 5 K on an EMX Plus continuous-wave X-band spectrometer (Bruker) with an ESR910 helium-flow cryostat (Oxford Instruments) and a dual-mode cavity (Bruker). Differential pulse voltammograms were measured with an ALS612A electrochemical analyzer (BAS). A saturated calomel reference electrode, a glassy carbon working electrode, and a platinum-wire counter electrode were utilized. Measurements were carried out for the 1 mM solution in anhydrous CH_2Cl_2 containing 0.1 M Bu_4NClO_4 at a scan rate of 50 mV s^{-1} at 203 K. The E values were referenced to that of ferrocene, which was measured under identical conditions. O_3 gas was prepared by UV irradiation to the O_2 gas, using a PR-1300 UV ozone generator (ClearWater Tech).

XAS Measurements. Mn K-edge XAS data were obtained at the SPring-8, beamline BL01B1, under ring conditions of 8 GeV and ca. 100 mA (Proposal No. 2007A1090). The XAS datum of **1** in the solid state was collected at room temperature, and the

XAS datum of the solution of **1**, *m*-CPBA, and Bu_4NOH in frozen propionitrile was collected at 10 K. The data collections were carried out in a fluorescence mode with a Lytle detector, using a Si(111) double-crystal monochromator. A copper foil was utilized to calibrate the energy. In each data collection, the first and final XAS data were carefully compared to confirm no appreciable X-ray damage on the sample. The XAS data were Fourier-transformed between $k = 2$ and 12 \AA^{-1} and processed in a standard manner by *WinXAS* software (version 3.1).³⁴ Theoretical EXAFS signals were calculated using *FEFF* (version 8.4).³⁵ Curve fittings were carried out only for atoms that are coordinated to manganese.

Materials. CH_2Cl_2 was purchased from Kanto as an anhydrous solvent and was stored in the presence of 4A molecular sieves. Propionitrile (99%) was purchased from Sigma-Aldrich and was used as received. *m*-CPBA was purchased from Nacalai and was purified by washing with a phosphate buffer. The purity of *m*-CPBA was checked with iodometry. The synthesis of **1** was reported elsewhere.¹⁷ 2,6-Di-*tert*-butylphenol, 2,4-di-*tert*-butylphenol, and 2,4,6-tri-*tert*-butylphenol were purchased from Tokyo Chemical Industry and were used as received. 2,6-Di-*tert*-butyl-4-methylphenol was purchased from Sigma-Aldrich and was used as received. 3',5'-Di-*tert*-butyl-4'-hydroxyacetophenone and 3,5-di-*tert*-butyl-4-hydroxybenzonitrile were purchased from Alfa Aesar and were used as received. D_2O (99.8% D) was purchased from Acros and was purified by distillation under an argon atmosphere before use. 2,6-Di-*tert*-butylphenol-*d* was prepared by evaporation of a solution of 2,6-di-*tert*-butylphenol (1 g) dissolved in CH_3CN (9 mL) and D_2O (1 mL), which was repeated three times. ^1H NMR shows that the degree of deuteration, which is quite sensitive to residual H_2O in a nonpolar chlorinated solvent, is $\sim 90\%$ in a CDCl_3 solvent, which was washed with D_2O and then dried over 4A molecular sieves. The k_2 and k_{obs} values upon reaction of $\text{Mn}^{\text{IV}}(\text{salen})(\text{O})$ and $\text{Mn}^{\text{IV}}(\text{salen})(\text{OH})$ with 2,6-di-*tert*-butylphenol-*d* were thus obtained in a CH_2Cl_2 solvent that was similarly preequilibrated with D_2O . Tris(2,4-dibromophenyl)aminium hexachloroantimonate was prepared according to the reported method³⁶ and was assayed with titration by ferrocene. **Caution!** The perchlorate salts used in this study are potentially explosive and should be handled in a small amount with great care.

Preparation of the Sample Solution for Characterization. A solution of 1.0 equiv of *m*-CPBA was added to a solution of **1** at 203 K. The resulting solution was kept for 5 min at 203 K. Then, a solution of 1.0 equiv of NMO or Bu_4NOH was slowly added. After 5 min at 203 K, the solution was subjected to physicochemical measurements. The experimental conditions are 0.5 mM in CH_2Cl_2 for UV–vis in a quartz cell ($l = 0.1$ cm), 1.0 mM in CH_2Cl_2 containing 0.1 M Bu_4NClO_4 for EPR, and 20 mM in propionitrile for XAS.

Reactions of $\text{Mn}^{\text{IV}}(\text{salen})(\text{O})$ and $\text{Mn}^{\text{IV}}(\text{salen})(\text{OH})$ with Substituted Phenols. $\text{Mn}^{\text{IV}}(\text{salen})(\text{O})$ was prepared by passing a stream of O_3 and O_2 (ca. 10 mL) through the CH_2Cl_2 solution

(31) Osako, T.; Ohkubo, K.; Taki, M.; Tachi, Y.; Fukuzumi, S.; Itoh, S. *J. Am. Chem. Soc.* **2003**, *125*, 11027–11033.

(32) Gardner, K. A.; Kuehnert, L. L.; Mayer, J. M. *Inorg. Chem.* **1997**, *36*, 2069–2078.

(33) Pratt, D. A.; Dilabio, G. A.; Mulder, P.; Ingold, K. U. *Acc. Chem. Res.* **2004**, *37*, 334–340.

(34) Ressler, T. J. *Synchrotron Radiat.* **1998**, *5*, 118–122.

(35) Ankudinov, A. L.; Bouldin, C. E.; Rehr, J. J.; Sims, J.; Hung, H. *Phys. Rev. B* **2002**, *65*, 104107–1–11.

(36) Schmidt, W.; Steckhan, E. *Chem. Ber.* **1980**, *113*, 577–585.

of **1** (51 μM , 2.05 mL) in a quartz cell ($l = 1$ cm), and then excess O_3 gas was purged by passing Ar gas (10 mL) at 203 K. $\text{Mn}^{\text{IV}}\text{-(salen)(OH)}$ was prepared by the addition of 1.0 equiv of tris(2,4-dibromophenyl)aminium hexachloroantimonate (0.105 μmol) in CH_2Cl_2 (20 μL) and then 1.0 equiv of Bu_4NOH (0.105 μmol) in CH_2Cl_2 (20 μL) to a CH_2Cl_2 solution of **1** (51 μM , 2.05 mL) in a quartz cell ($l = 1$ cm) at 203 K. After the formation of $\text{Mn}^{\text{IV}}\text{-(salen)(O)}$ or $\text{Mn}^{\text{IV}}\text{-(salen)(OH)}$ was confirmed by UV-vis, substituted phenols in CH_2Cl_2 (20 μL) were added. The resulting solution was stirred at 203 K, and UV-vis spectral changes were monitored.

Quantum Chemical Calculations. Quantum chemical calculations were performed using the *Gaussian03* program package.³⁷

(37) Frisch, M. J. *Gaussian03*, revision C.03; Gaussian, Inc.: Wallingford, CT, 2004.

The 6-311G(d) basis set was utilized for manganese, nitrogen, and oxygen atoms. The 6-31G(d) and STO-3G basis sets were utilized for the salen ligand and xylol substituents, respectively. The optimized structures were calculated using B3LYP density functional methods.

Acknowledgment. We thank Dr. Hajime Tanida (JASRI/SPRING-8) for assistance in the measurement of X-ray absorption spectra. We thank Prof. James M. Mayer for helpful comments. This work was supported by grants from the Japan Science and Technology Agency, CREST, and the Japan Science Promotion Society, the Global COE program.

Supporting Information Available: Figures S1–S15 and complete ref 37. This material is available free of charge via the Internet at <http://pubs.acs.org>.